Research Article | Vol. 33, No. 13 / 30 Jun 2025 / Optics Express 27236
Optics EXPRESS

Far-zone properties of a partially coherent field diffracted by a grating

MENGDI LI,[1] XIAOYAN PANG,[2] HUGO F. SCHOUTEN,[3] AND TACO D. VISSER[1,3,*]

[1]School of Physics and Electronics, Shandong Normal University, Jinan 250358, China
[2]School of Electronics and Information, Northwestern Polytechnical University, Xi'an, China
[3]Dept. of Physics and Astronomy, Vrije Universiteit, Amsterdam, The Netherlands
[*]tvisser@nat.vu.nl

Abstract: We study the diffraction of a partially coherent beam by a transmission grating. Both the state of coherence and the angular intensity distribution of the far-zone field are found to be dependent on the intensity width as well as the coherence width of the incident beam. Typically, the angular intensity distribution broadens with decreasing coherence, whereas all the diffraction orders remain fully correlated.

1. Introduction

Various types of diffraction gratings [1] are routinely used in both quantum optics [2] and classical optics [3], and in applications such as spectroscopy [4], remote sensing [5], and pulse stretching and compression [6]. Unlike the situation that is commonly described in textbooks [7], quite often the incident field is not fully coherent. One of many examples is active remote sensing in which a satellite sends out a laser beam to the surface of the Earth and then uses a grating to analyze the back-reflected signal. Even though the beam starts out as spatially fully coherent, the passage through atmospheric turbulence will render it partially coherent [8]. It is remarkable therefore, that very few studies have been dedicated to gratings receiving partially coherent light. Among them is [9], a preliminary analysis of the effects of spatial coherence on possible spectral changes in the far-zone. However, that study presents no closed-form expressions or numerical results. In [10] the influence of temporal coherence on the intensity distribution in successive Talbot planes was examined. The van Cittert-Zernike theorem was generalized for weakly periodic media in [11]. A numerical study of near-field changes in spatial coherence induced by a metal grating was presented in [12]; and in [13] a super-oscillatory behavior of the spatial correlation function was described. Most recently, the generation of so-called *coherence carpets* in the Fresnel zone was predicted in [14].

In the present study the diffraction of a spatially partially coherent beam by a transmission grating is analyzed. The resulting formulas are illustrated for the case of a Gaussian-correlated beam with a Gaussian intensity profile, which is diffracted by an amplitude grating. We report two contributions. First, we derive formulas that describe the effects of spatial coherence on the angular far-zone intensity distribution and the spectral degree of coherence. Second, we find for Gaussian beams with a Gaussian correlation that in the far zone the correlation between the different diffraction orders peaks around their respective intensity maximum. Both the intensity and the coherence of the diffracted field are determined by an interplay of the intensity width and the coherence width of the incident beam.

2. Coherence-induced changes of the far-zone field

We consider a transmission grating with period L that is invariant along the y-direction and which is situated in the plane $z = 0$ (see Fig. 1). The incident field, denoted $U^{(\mathrm{in})}(x, \omega)$, with x a position

#566888 https://doi.org/10.1364/OE.566888
Journal © 2025 Received 1 May 2025; revised 9 Jun 2025; accepted 10 Jun 2025; published 17 Jun 2025

Optics EXPRESS

and ω an angular frequency, propagates in the positive z-direction. The field is assumed to be partially coherent, and invariant along y. Its cross-spectral density (CSD) function, the two-point correlation function that describes its statistical properties in the space-frequency domain, is defined as [15]

$$W^{(\mathrm{in})}(x_1, x_2, \omega) = \langle U^{(\mathrm{in})*}(x_1, \omega) U^{(\mathrm{in})}(x_2, \omega) \rangle, \tag{1}$$

where the angled brackets indicate an ensemble average. For brevity we suppress the frequency dependence of the various quantities in the remainder. The transmitted field immediately behind the grating, denoted $U^{(\mathrm{out})}(x)$, equals

$$U^{(\mathrm{out})}(x) = t(x) U^{(\mathrm{in})}(x), \tag{2}$$

where $t(x)$ is the grating transmission function. The CSD function of this field thus becomes

$$W^{(\mathrm{out})}(x_1, x_2) = t^*(x_1) t(x_2) W^{(\mathrm{in})}(x_1, x_2). \tag{3}$$

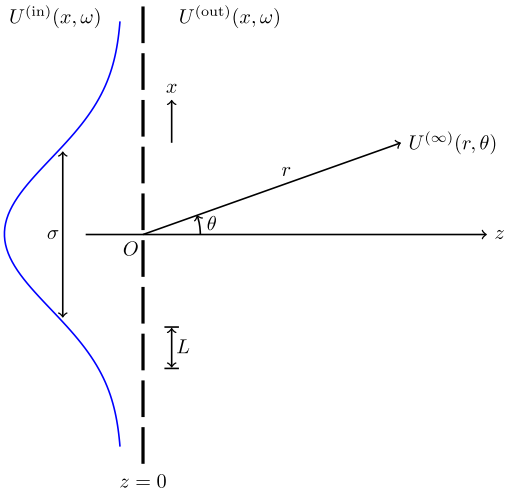

Fig. 1. Illustrating the geometry and notation.

Because the grating has period L, the transmission function can be written as a Fourier series, i.e. [16]

$$t(x) = \sum_{n=-\infty}^{\infty} c_n \mathrm{e}^{\mathrm{i}2\pi n x/L}, \tag{4}$$

with

$$c_n = \frac{1}{L} \int_L t(x) \mathrm{e}^{-\mathrm{i}2\pi n x/L} dx, \tag{5}$$

and where the integration is over any interval with length L. Substitution from Eq. (4) into Eq. (3) yields

$$W^{(\mathrm{out})}(x_1, x_2) = \sum_{n,m} c_n^* c_m \mathrm{e}^{-\mathrm{i}2\pi n x_1/L} \mathrm{e}^{\mathrm{i}2\pi m x_2/L} W^{(\mathrm{in})}(x_1, x_2). \tag{6}$$

The incident beam is centered around the z-axis and illuminates a finite portion of the grating. At a sufficiently large distance behind the grating, the forward-diffracted field in the vicinity of

Optics EXPRESS

the z-axis is [17]

$$U(x,z) = C\int_{-\infty}^{\infty} U^{(\mathrm{out})}(x')\frac{\mathrm{e}^{\mathrm{i}kR}}{\sqrt{R}}\,dx', \tag{7}$$

where C is a constant and R is the distance from $(x',0)$ to (x,z). In the remainder, unless otherwise specified, all integrals are assumed to range from $-\infty$ to ∞. We are interested in the far-zone field, denoted by $U^{(\infty)}$. Using polar coordinates, the far-zone form of Eq. (7) may be approximated as

$$U^{(\infty)}(r,\theta) \approx \frac{C\mathrm{e}^{\mathrm{i}kr}}{\sqrt{r}}\int U^{(\mathrm{out})}(x')\mathrm{e}^{-\mathrm{i}kx'\sin\theta}\,dx', \tag{8}$$

where the r is the distance from $(0,0)$ to (x,z), and θ represents the polar angle. On defining the one-dimensional spatial Fourier transform as

$$\tilde{U}^{(\mathrm{out})}(f) = \int U^{(\mathrm{out})}(x')\mathrm{e}^{-\mathrm{i}fx'}\,dx', \tag{9}$$

Equation (8) can be cast in the more compact form

$$U^{(\infty)}(r,\theta) = \frac{C\mathrm{e}^{\mathrm{i}kr}}{\sqrt{r}}\tilde{U}^{(\mathrm{out})}(k\sin\theta). \tag{10}$$

The CSD function of the far-zone field is defined, in strict analogy with Eq. (1), as

$$\begin{aligned} W^{(\infty)}(r_1,\theta_1,r_2,\theta_2) &= \langle U^{(\infty)*}(r_1,\theta_1)U^{(\infty)}(r_2,\theta_2)\rangle = \frac{|C|^2\mathrm{e}^{\mathrm{i}k(r_2-r_1)}}{\sqrt{r_1r_2}} \\ &\times\left\langle\int U^{(\mathrm{out})*}(x_1')\mathrm{e}^{\mathrm{i}kx_1'\sin\theta_1}dx_1'\int U^{(\mathrm{out})}(x_2')\mathrm{e}^{-\mathrm{i}kx_2'\sin\theta_2}dx_2'\right\rangle. \end{aligned} \tag{11}$$

Next we introduce the two-dimensional Fourier transform

$$\tilde{W}^{(\mathrm{out})}(f_1,f_2) = \iint W^{(\mathrm{out})}(x_1',x_2')\mathrm{e}^{-\mathrm{i}(f_1x_1'+f_2x_2')}dx_1'dx_2'. \tag{12}$$

On interchanging the order of integration and ensemble averaging in Eq. (11), it may be rewritten as

$$W^{(\infty)}(r_1,\theta_1,r_2,\theta_2) = \frac{|C|^2\mathrm{e}^{\mathrm{i}k(r_2-r_1)}}{\sqrt{r_1r_2}}\tilde{W}^{(\mathrm{out})}(-k\sin\theta_1,k\sin\theta_2). \tag{13}$$

The spectral density (or 'intensity at frequency ω') in the far-zone is given by the CSD function at two coincident points [15], i.e.,

$$S^{(\infty)}(r,\theta) = W^{(\infty)}(r,\theta,r,\theta), \tag{14}$$

and hence

$$S^{(\infty)}(r,\theta) = \frac{|C|^2}{r}\tilde{W}^{(\mathrm{out})}(-k\sin\theta,k\sin\theta). \tag{15}$$

The normalized version of the CSD function, the spectral degree of coherence [15], is defined as

$$\mu^{(\infty)}(r_1,\theta_1,r_2,\theta_2) \equiv \frac{W^{(\infty)}(r_1,\theta_1,r_2,\theta_2)}{\sqrt{S^{(\infty)}(r_1,\theta_1)S^{(\infty)}(r_2,\theta_2)}}. \tag{16}$$

The spectral degree of coherence is bounded between zero and unity, where zero represents a completely incoherent field and unity a field that is fully coherent. For intermediate values the field is said to be partially coherent. The spectral degree of coherence is a measure of the visibility of interference fringes that are formed in Young's experiment [18].

Thus far, no assumptions were made about the CSD function of the incident field or the precise geometry of the grating. In the next section we illustrate the effects of spatial coherence for a specific case.

Optics EXPRESS

3. Intensity of the far-zone field

We assume an incident beam with an intensity profile and a homogeneous correlation that both are of a Gaussian form, i.e.,

$$W^{(\mathrm{in})}(x_1, x_2) = A_0^2 \, \mathrm{e}^{-(x_1^2+x_2^2)/(4\sigma^2)} \, \mathrm{e}^{-(x_2-x_1)^2/(2\delta^2)}, \tag{17}$$

with A_0 the amplitude, σ the width, and δ the coherence width (or 'coherence radius') of the beam (see Fig. 1). On substituting into Eqs. (6) and (12) and changing to sum and difference variables, the double integral factorizes, giving the result

$$\begin{aligned} \tilde{W}^{(\mathrm{out})}(f_1, f_2) = 2\pi A_0^2 \sigma \Omega \sum_{n,m} c_n^* c_m \, \mathrm{e}^{-[2\pi(m-n)/L - f_1 - f_2]^2 \sigma^2/2} \\ \times \mathrm{e}^{-[\pi(m+n)/L + (f_1-f_2)/2]^2 \Omega^2/2}, \end{aligned} \tag{18}$$

where we introduced

$$\frac{1}{\Omega^2} = \frac{1}{4\sigma^2} + \frac{1}{\delta^2}. \tag{19}$$

We thus obtain for the far-zone CSD function the expression

$$\begin{aligned} W^{(\infty)}(r_1, \theta_1, r_2, \theta_2) = \frac{|C|^2}{\sqrt{r_1 r_2}} 2\pi A_0^2 \sigma \Omega \, \mathrm{e}^{\mathrm{i}k(r_2 - r_1)} \sum_{n,m} c_n^* c_m \\ \times \mathrm{e}^{-[2\pi(m-n)/L + k\sin\theta_1 - k\sin\theta_2]^2 \sigma^2/2} \\ \times \mathrm{e}^{-[\pi(n+m)/L - (k\sin\theta_1 + k\sin\theta_2)/2]^2 \Omega^2/2}. \end{aligned} \tag{20}$$

Making use of this in Eq. (14) for the far-field spectral density gives

$$S^{(\infty)}(r, \theta) = \beta \sum_{n,m} c_n^* c_m \mathrm{e}^{-[2\pi(m-n)/L]^2 \sigma^2/2} \mathrm{e}^{-[\pi(m+n)/L - k\sin\theta]^2 \Omega^2/2}, \tag{21}$$

where $\beta = |C|^2 2\pi A_0^2 \sigma \Omega / r$.

Under typical circumstances several slits will be illuminated, meaning that the beam width σ is larger than the grating period L. In that case only the $m = n$ term gives a significant contribution, and Eq. (21) reduces to a single sum, i.e.,

$$S^{(\infty)}(r, \theta) = \beta \sum_{n} |c_n|^2 \mathrm{e}^{-[\frac{2\pi n}{L} - k\sin\theta]^2 \Omega^2/2}, \quad \sigma > L. \tag{22}$$

This expression has a clear physical interpretation. It describes the far-zone spectral density as a sum of diffraction orders, with label n, which are Gaussian angular distributions that attain their respective maximum in a direction θ_n such that

$$L \sin\theta_n = n\lambda, \quad n = 0, \pm 1, \pm 2, \ldots \tag{23}$$

which is the angle given by the classical grating equation for a uniform and spatially fully coherent illumination [19, Sec. 8.6]. Hence, compared to the 'traditional case', a Gaussian beam with a homogeneous Gaussian correlation has the same angular maxima. However, the diffraction orders are seen to be broadened due to the finite values of the coherence radius δ and the beam width σ, which are both contained in the factor Ω. This broadening obviously reduces the resolving power of the grating.

Optics EXPRESS

We illustrate the implications of Eq. (22) for the case of an amplitude grating. For such a grating the transmission $t(x) = 1$ within the slits and 0 elsewhere. We assume that the slits are located symmetrically around $x = 0$, and hence [16]

$$c_n = \frac{b}{L}\mathrm{sinc}\left(\frac{n\pi b}{L}\right), \tag{24}$$

where b is the slit width.

The angular intensity distribution, as calculated from Eq. (22), is presented in Fig. 2 for two different amplitude gratings. The top panel is for a grating with $L = 20\lambda$ and $b = 4\lambda$; the bottom panel is for $L = 20\lambda$ and $b = 10\lambda$ (i.e., a Ronchi grating). The red curves represent the case $\delta = 200\lambda$, and shows sharp diffraction orders. When the coherence radius decreases to 25λ (blue curves) the intensity distributions become significantly broader. When δ is further reduced to 10λ, the different orders overlap (green curves). For the Ronchi grating shown in the bottom panel, the second and fourth diffraction orders are suppressed because in that case $c_2 = c_4 = 0$.

When the diffraction orders do not overlap, i.e., when $\delta > L$ (as for the red and blue curves of Fig. 2), one can define the total power scattered into order n as the contribution of just the n^{th} term in Eq. (22), i.e.,

$$S_n^{(\infty)} \equiv \beta|c_n|^2 \int_{-\infty}^{\infty} \mathrm{e}^{-[2\pi n/L - k\sin(\theta_n + d\theta)]^2\Omega^2/2}\, d\theta, \tag{25}$$

with θ_n the angle of maximum intensity of the order, as given by Eq. (23), and where we have formally extended the limits of integration. Using a small-angle approximation one can show that

$$S_n^{(\infty)} = \frac{|C|^2(2\pi)^{3/2}A_0^2\sigma}{kr}|c_n|^2, \quad \delta > L. \tag{26}$$

This result shows that the relative total power contained in the n^{th} order is independent of the coherence width δ, and is proportional to $|c_n|^2$. This latter factor, as is seen from Eq. (24), is determined solely by the grating geometry. We emphasize that this result is obtained under the assumption of the illumination and the correlation both being Gaussian.

4. Coherence of the far-zone field

Next we analyze the correlation properties of the field scattered into the vicinity of two intensity maxima. We start with Eq. (20) while setting

$$\theta_1 = \theta_p + d\theta_1, \quad \text{with } L\sin\theta_p = p\lambda, \tag{27}$$

$$\theta_2 = \theta_q + d\theta_2, \quad \text{with } L\sin\theta_q = q\lambda, \tag{28}$$

and p and q both integers [see Eq. (23)]. Using that $\sin\theta_1 \approx \sin\theta_p + d\theta_1$, with a similar expression for $\sin\theta_2$, we find that

$$\begin{aligned} W^{(\infty)}(r_1,\theta_1,r_2,\theta_2) = B\sum_{n,m} c_n^* c_m \mathrm{e}^{-[2\pi(m-n+p-q)/L + k(d\theta_1 - d\theta_2)]^2\sigma^2/2} \\ \times \mathrm{e}^{-[\pi(n+m-p-q)/L - k(d\theta_1 + d\theta_2)]^2\Omega^2/2}, \end{aligned} \tag{29}$$

where $B = |C|^2 2\pi A_0^2\sigma\Omega\,\mathrm{e}^{\mathrm{i}k(r_2-r_1)}/(r_1 r_2)^{1/2}$. As before, since typically the beam width σ is greater than the period L, the first exponential in the summation is only non-negligible if $n = m + p - q$,

Optics EXPRESS

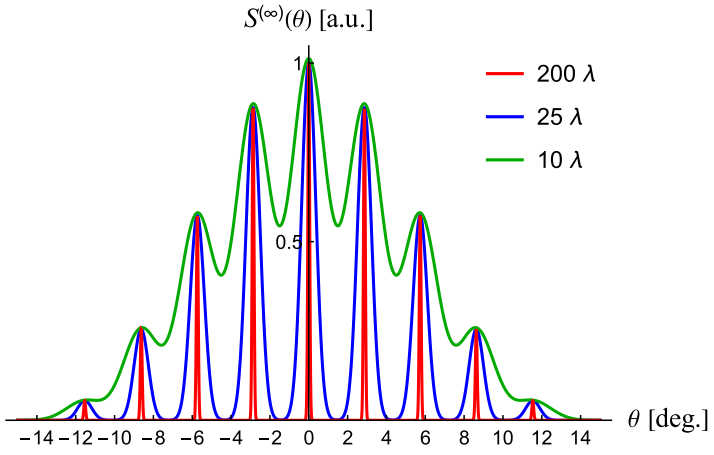

(a) Periodicity $L = 20\lambda$, slit width $b = 4\lambda$.

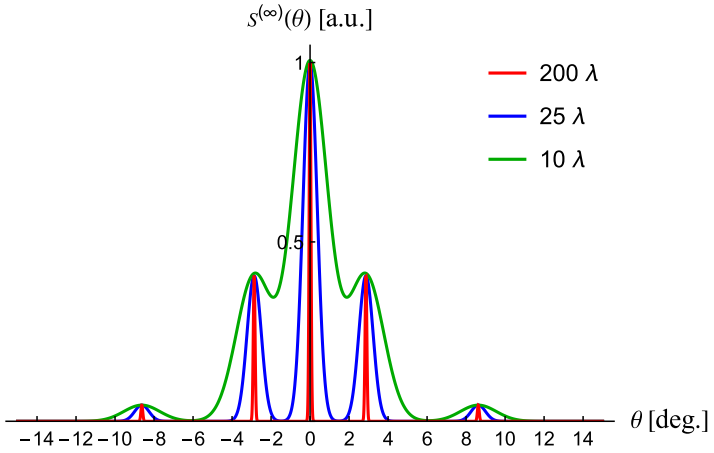

(b) Periodicity $L = 20\lambda$, slit width $b = 10\lambda$.

Fig. 2. The far-zone intensity produced by two gratings for three different values of the coherence width δ. Red: $\delta = 200\lambda$, blue: $\delta = 25\lambda$, and green: $\delta = 10\lambda$. The top panel is for a grating with $L = 20\lambda$ and $b = 4\lambda$. The bottom panel is for $L = 20\lambda$ and $b = 10\lambda$. In both cases the beam width $\sigma = 400\lambda$.

where it is assumed that $kd\theta_i \ll 2\pi/L$, for $i = 1, 2$. Hence we can write

$$W^{(\infty)}(r_1, \theta_1, r_2, \theta_2) = B \sum_m c^*_{m+p-q} c_m \mathrm{e}^{-k^2(d\theta_1 - d\theta_2)^2\sigma^2/2} \times \mathrm{e}^{-[2\pi(m-q)/L - k(d\theta_1 + d\theta_2)/2]^2\Omega^2/2}. \tag{30}$$

If in addition we also have that the coherence length $\delta > L$, then $\Omega > L$, and the summation further reduces to a single term, i.e., $m = q$, and

$$W^{(\infty)}(r_1, \theta_1, r_2, \theta_2) = B c^*_p c_q \mathrm{e}^{-k^2(d\theta_1 - d\theta_2)^2\sigma^2/2} \mathrm{e}^{-k^2(d\theta_1 + d\theta_2)^2\Omega^2/8}. \tag{31}$$

As an aside, the effects of a δ-correlated field are discussed in [14]. On substituting from Eqs. (31) and (22) into the definition (16) of the spectral degree of coherence, we find for its

Optics EXPRESS

magnitude that

$$|\mu^{(\infty)}(r_1,\theta_1,r_2,\theta_2)| = \mathrm{e}^{-k^2(d\theta_1-d\theta_2)^2(\sigma^2-\Omega^2/4)/2} \tag{32}$$

$$= \mathrm{e}^{-k^2(\theta_1-\theta_p-\theta_2+\theta_q)^2(\sigma^2-\Omega^2/4)/2}, \quad \sigma,\delta>L, \tag{33}$$

which is independent of our choice of diffraction orders p and q. One immediate consequence of Eq. (32) is that in the far zone the modulus of the spectral degree of coherence is unity whenever $d\theta_1 = d\theta_2$. As a special case, this means that the maxima of any two diffraction orders (for which $d\theta_1 = d\theta_2 = 0$) are fully correlated with one another. Apparently, after diffraction by the grating, a partially coherent incident field becomes fully coherent on propagation to the far-zone. This result can be understood by noting that the different diffraction orders all represent the same field superposition, apart from a path difference that is precisely an integer number of wavelengths and which is therefore of no consequence.

We can rewrite Eq. (33) as

$$|\mu^{(\infty)}(r_1,\theta_1,r_2,\theta_2)| = \mathrm{e}^{-k^2(\theta_1-\theta_p-\theta_2+\theta_q)^2\Gamma^2/2}, \tag{34}$$

with

$$\frac{1}{\Gamma^2} = \frac{1}{\sigma^2}\left(1+\frac{\delta^2}{4\sigma^2}\right). \tag{35}$$

The factor Γ for the width of the spectral degree of coherence is to be compared with its counterpart Ω for the intensity width [see Eq. (22)]. One can derive that both widths are only equal if $\delta = \sigma$. Two cases are illustrated in Fig. 3, in which both $|\mu^{(\infty)}(r_1,\theta_1,r_2,0)|$ and $S^{(\infty)}(\theta_1)$ are plotted. In panel (a), with $\sigma>\delta$, it is seen that within each diffraction order the coherence width is significantly smaller than the intensity distribution. In panel (b), with $\sigma<\delta$, the opposite occurs. Now the angular coherence width is significantly larger than the intensity width. For the choice of parameters in Fig. 3 the curves based on the approximate expressions (33) and (22), are in excellent agreement with those of the double-sum formulas (29) and (21). We note that the behavior of the far-zone spectral degree of coherence as given by Eq. (34) is independent of the slit width b.

A case of practical interest is that of an incident beam that is quasi-homogeneous, i.e., a beam with $\sigma^2 \gg \delta^2$, and hence [from Eq. (19)] $\Omega^2 \approx \delta^2$, and [from Eq. (35)] $\Gamma^2 \approx \sigma^2$. This means that for such a beam the width of the far-zone diffraction orders, given by Eq. (22), is mainly governed by the coherence width δ, whereas the width of the spectral degree of coherence, given by Eq. (34), is mainly governed by the beam width σ. Such a role reversal of these two parameters also occurs in the reciprocity relations for quasi-homogeneous sources and their far-zone fields [15, Sec. 5.3.2].

5. Discussion and conclusions

It is well known that the state of spatial coherence of a wave field determines how it propagates [20] and how it scatters [21]. However, the effects of coherence on grating diffraction have until now received much less attention. Here we have analyzed the often occurring case of a spatially partially coherent beam passing through an amplitude grating. Expressions for the far-zone state of coherence and the intensity were derived. The individual diffraction orders were seen to be broadened, due to an interplay of the beam's intensity width and its coherence width, as captured by the parameter Ω.

All the diffraction order maxima were found to be fully correlated. However, within each order the coherence drops off following a Gaussian function. It is worth contrasting this result with the van Cittert-Zernike theorem [15], according to which a *completely incoherent* source generates a *partially coherent* far-zone field.

Optics EXPRESS

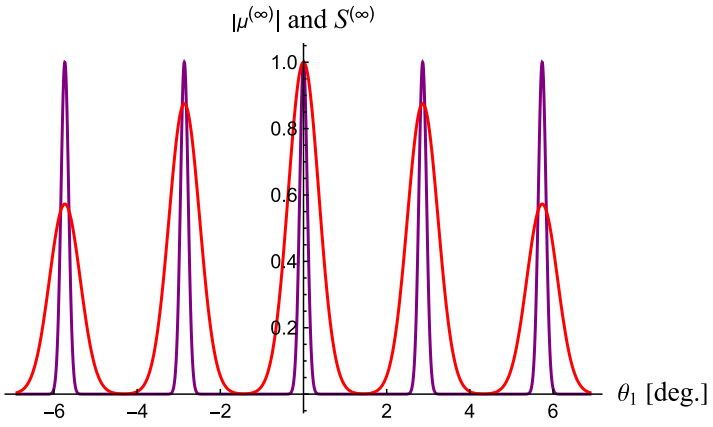

(a) Beam width $\sigma = 100\lambda$, coherence width $\delta = 25\lambda$.

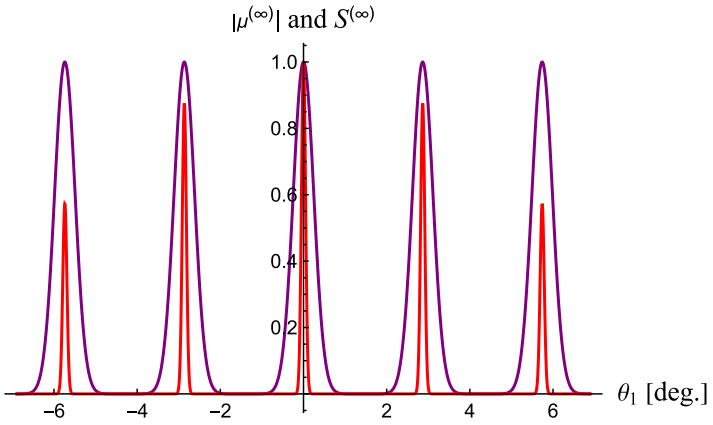

(b) Beam width $\sigma = 100\lambda$, coherence width $\delta = 500\lambda$.

Fig. 3. The spectral degree of coherence $|\mu^{(\infty)}|$ (purple curve) and the normalized intensity $S^{(\infty)}$ (red curve) for a grating with $L = 20\lambda$ and $b = 4\lambda$. The beam width $\sigma = 100\lambda$ in both panels. In (a) $\delta = 25\lambda$, in (b) $\delta = 500\lambda$.

The broadening of diffraction orders as described here, has a direct consequence for the spectral resolving power of gratings. Furthermore, we expect our result to be relevant for the many applications, among them LIDAR, in which a transmission grating is used to analyze a partially coherent field.

Possible generalizations of this work are the extension to phase gratings, to Bessel-correlations, in which correlations can be negative [22]; and to electromagnetic fields, in order to include polarization effects.

Funding. National Natural Science Foundation of China (W2441005); Key Research and Development Projects of Shaanxi Province (2024GX-YBXM-080); Fundamental Research Funds for the Central Universities (D 5000240290).

Disclosures. The authors declare no conflicts of interest.

Data availability. No data were generated in this study.

Optics EXPRESS

References

1. C. Palmer, *Diffraction Grating Handbook*, 8th ed. (MKS Instruments, 2020).
2. M. S. Chapman, C. R. Ekstrom, T. D. Hammond, *et al.*, "Near-field imaging of atom diffraction gratings: The atomic Talbot effect," Phys. Rev. A **51**(1), R14–R17 (1995).
3. W. B. Case, M. Tomandl, S. Deachapunya, *et al.*, "Realization of optical carpets in the Talbot and Talbot-Lau configurations," Opt. Express **17**(23), 20966–20974 (2009).
4. I. A. Zarubin, V. A. Labusov, and S. A. Babin, "Characteristics of compact spectrometers with diffraction gratings of different types," Inorg. Mater. **56**(14), 1436–1440 (2020).
5. Y. Lu, B. Li, Y. Zheng, *et al.*, "Polarization-insensitive two-dimensional reflective grating with high-diffraction efficiency for space-borne CO_2 imaging spectrometer," Opt. Laser Technol. **167**, 109762 (2023).
6. D. Strickland and G. Mourou, "Compression of amplified chirped optical pulses," Opt. Commun. **56**(3), 219–221 (1985).
7. E. Popov, (ed.), *Gratings: Theory and Numeric Applications*, 2nd revised edition (Institut Fresnel, 2014). See: www.fresnel.fr/numerical-grating-book-2.
8. P. Barcik and L. Hudcova, "Measurement of spatial coherence of light propagating in a turbulent atmosphere," Radioengineering **22**, 341–345 (2013).
9. M. Dušek, "Diffraction grating illuminated by partially coherent beam," Opt. Commun. **111**(3-4), 203–208 (1994).
10. S. Teng, L. Liu, J. Zu, *et al.*, "Uniform theory of the Talbot effect with partially coherent light illumination," J. Opt. Soc. Am. A **20**(9), 1747–1754 (2003).
11. B. J. Hoenders and M. Bertolotti, "Theory of partial coherence for weakly periodic media," J. Opt. Soc. Am. A **22**(12), 2682–2690 (2005).
12. T. Saastamoinen and H. Lajunen, "Increase of spatial coherence by subwavelength metallic gratings," Opt. Lett. **38**(23), 5000–5003 (2013).
13. J. Mays and G. Gbur, "Partially coherent superoscillations in the Talbot effect," J. Phys. A: Math. Theor. **55**(50), 504002 (2022).
14. H. F. Schouten and T. D. Visser, "Gratings weave coherence carpets with non-diffracting coherence strands," Optica **12**(5), 708–712 (2025).
15. E. Wolf, *Introduction to the Theory of Coherence and Polarization of Light* (Cambridge University Press, 2007).
16. G. B. Arfken and H. J. Weber, *Mathematical Methods for Physicists*, 6thed. (Elsevier, 2005). See Ch. 14.
17. B. B. Baker and E. T. Copson, *The Mathematical Theory of Huygens' Principle* (Chelsea Publishing, 1987).
18. G. Gbur and T. D. Visser, "Young's interference experiment: Past, present, and future," in: *Progress in Optics*, vol. 67, pp. 275–343 (Elsevier, 2022).
19. M. Born and E. Wolf, *Principles of Optics*, 7th ed. (Cambridge University Press, 1999).
20. O. Korotkova and E. Wolf, "Changes in the state of polarization of a random electromagnetic beam on propagation," Opt. Commun. **246**(1-3), 35–43 (2005).
21. H. F. Schouten and T. D. Visser, "Scattering of partially coherent electromagnetic beams by a sphere," Opt. Express **32**(6), 10690–10702 (2024).
22. T. van Dijk, G. Gbur, and T. D. Visser, "Shaping the focal intensity distribution using spatial coherence," J. Opt. Soc. Am. A **25**(3), 575–581 (2008).